We thank **Referee #2** (K. Lamb) for reviewing the manuscript, and for his thorough recommendations to improve the paper. Appropriate changes will be included in a future version of the revised manuscript, according to detailed responses to each of the referee's concerns (below with referee's comments in italic).

Points raised by referee #2:

1. There are a number of places where the English could be improved.

R: We appreciate all the referee's notes, and changes will be made as instructed. In particular, for points (e), (h) and (x) please note that:

> *(e) page 3, line 23: how does satellite altimetry confirm that IWs transport mass?*
>
> **R**: We acknowledge that this sentence may be confusing, since satellite altimetry is confirming only the long propagations distances for the internal tides. The sentence will be rewritten and read: "Satellite altimetry studies (see e.g. Ray and Cartwright, 2001) have indeed confirmed propagating distances of the order of 1000 km for the long Internal Tides (ITs, i.e. IWs of tidal frequency), and shorter-scale Internal Solitary Waves (ISWs) have been shown by other remote sensing methods to propagate considerable distances as well (e.g. da Silva et al., 2011; Guo et al., 2012)".
>
> *(h) page 4, line 16: what is meant be 'admittedly' here? Do you mean 'presumably'.*
>
> **R**: We agree that 'presumably' conveys the appropriate meaning (and not 'admittedly'), since these energy transfers to smaller-scale waves were only suggested based on visual observations made by the crew.
>
> *(x) page 20, line 5: what is mean by Ht performing?*
>
> **R**: The term will be replaced by 'decreasing' so that the sentence will read: "… with Ht decreasing accordingly (see blue line in Fig. 12a)."

2. I think it would be helpful to give more information on water depths where the waves are observed.

R: We agree we the referee and depth contours for 200, 500, 1000, 2000, 3000, 4000, and 4500 m have been added in thin grey lines to Fig. 9a (see new version in attached file). Note the 200m and 1000m contours are hardly distinguishable from the 500 m isobath (highlighted in a black thick line), and thus representative of a steep shelf-break, where the waves are believed to be generated.

3. Page 13, equation (3). Should be $\phi(-H) = 0$.

R: Eq. (3) will be corrected as instructed in the revised version of the manuscript.

4. ISW widths are given in Figure 6. How exactly was the wave width defined?

R: The characteristic soliton widths presented in Fig. 6 are defined from their corresponding SAR sea surface signatures, as shown in Fig. 4a (labelled '*L*') for a normalized backscatter intensity profile taken across a representative solitary wave shown in Fig. 3b. This is a typical parameter estimated in SAR studies involving ISWs (see e.g. New and da Silva, 2002; da Silva et al., 2011), which is meant as a measure of the individual waves horizontal scales (along their propagation direction). It is important to note that ISWs propagating on the near surface thermocline (or pycnocline) are capable of producing sea surface roughness patterns that are observable by satellite-borne SARs when the wind speed is not excessively strong (e.g. Alpers, 1985). A schematic view is shown in Fig. R1 (bellow), according to hydrodynamic modulation theory (as described in Alpers, 1985), where it can be seen how the isopycnal displacements below (and corresponding dimensions) translate to the SAR images above. According to this figure, mode-1 ISW interfacial waves travelling along the pycnocline (assuming waves of depression, which is often the case in deep waters) will be revealed in SAR images by bright bands preceding darker ones in their direction of travel. In essence, this follows from surface velocity fields induced by travelling ISWs, which create different convergence and divergence patterns, modulating the surface roughness and thus the intensity of the radar backscatter signal. In practice, however, ISW sea surface signatures are modulated by other ambient factors, such as the local wind speed and direction, the presence of organic surface films, and possible resonant interaction with surface waves (see Alpers, 1985; da Silva et al., 1998; Brandt et al., 1999; Araújo et al., 2002; and Kudryavtsev et al., 2005 for a detailed discussion). In these cases the SAR intensity variations, which are usually symmetrically distributed about a mean value close to zero, can be shifted towards more positive or negative values depending if the waves are seen as bright bands in a darker background or vice-versa. Therefore, all our estimates for *L* yield only a proxy for the waves' horizontal dimensions. Further notes, conveying a summary of the above information will be inserted in the text (along with appropriate references), as additional information to clarify this issue for the broader oceanographic community.

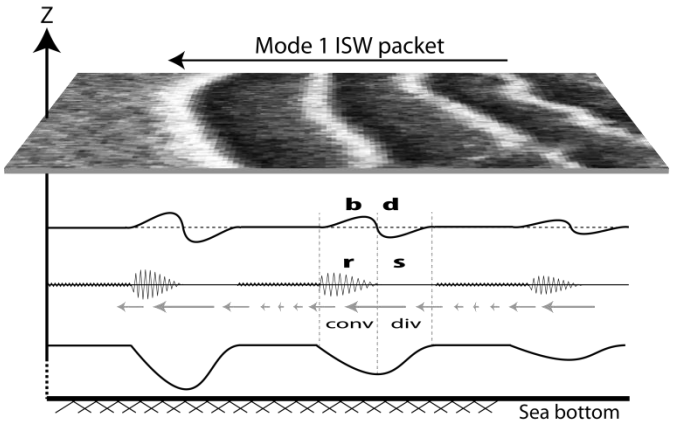

Figure R1. Example of a SAR image showing sea surface signatures of a mode-1 ISW packet. The ISWs are assumed to be moving from right to let. From top to bottom the horizontal profiles represent the following features: SAR intensity profile along the ISWs, with bright enhanced backscatter (b) preceding dark reduced backscatter (d) in the direction of propagation; surface roughness representation indicating how rough (r) and smooth (s) the surface is along an ISW wave packet; surface current variability induced by ISWs (note indication of convergence and divergence fields near the surface); isopycnal displacements produced by ISW propagation.

5. Referring to HYCOM simulations 6.1 and 18.5 is not very informative. I don't see any value if even mentioning 'simulation 6.1'. Can you give more information regarding resolution, how long the simulation was for, does it include the NECC and the North Brazilian Current etc.?

R: Terminologies including solutions 6.1 and 18.5 (i.e. concerning the HYCOM simulations) will be removed from the text, keeping only the corresponding references. We agree with the referee in adding further details concerning the HYCOM simulations used in paper. These will be included in the text, summarizing that HYCOM is a realistically forced three-dimensional global ocean model (3D global HYbrid Coordinate Ocean Mode, see Bleck 2002), with both tidal and atmospheric forcing, and hence including the ocean's major current systems, such as the NBC or the NECC. The simulations used in this manuscript refer to an annual period (from October 2011 to September 2012) and their tidal forcing includes the largest semi-diurnal and diurnal constituents (i.e. M_2, S_2, N_2, K_2, and K_1, O_1, P_1, Q_1), where a nominal horizontal resolution is set to 1/12° at the equator with 32 layers in the vertical direction. Hourly 3D time series were monthly averaged, whereas Fig. 10 displays the depth integrated and time-mean (over one full year) conversion rates (C, left panel) and energy fluxes ($\mathbf{F}_E$, right panel) for the filtered semi-diurnal tides. A more detailed description of the HYCOM simulations used in this paper may be found in Buijsman et al. (2015) and references therein (see also Metzger et al., 2010 and Shriver et al., 2012).

6. Page 16, first paragraph. Is there a reason for the reduced generation between generation sites A and B? Reduced tidal currents?

R: A tidal ellipse map computed from a regional solution (using the Oregon Tidal Prediction Software, OTIS, at a resolution of 1/12°, see Egbert and Erofeeva, 2002) is presented in Fig. R2. No significant changes in the along-shelf tidal ellipses can be seen, in particular in between A and B. We note these ellipses are representative of neap-tides, whereas a similar view still holds for spring tides. However, the weaker conversion rates given at the promontory near

315.5°E and 0°N (see our Fig. 10a) are in fact consistent with our SAR observations, which show no significant ISW activity in between A and B. Therefore, at this point, we prefer to discuss the separation between distinct generation sites A and B on the basis of the conversion rates yielded by the HYCOM simulations, since these systematically (i.e. throughout the year) present similar results to those present in Fig. 10a. Nonetheless, we appreciate raising this particular aspect of the study region and possible reasons, such as the convex (as seen from the open ocean) geometry of the promontory (scattering energy rather than focusing it), are set to be further investigated within forthcoming 2D high-resolution simulations in several across-shelf transects between A and B, as well as in the frame of 3D configurations (using the fully nonlinear and non-hydrostatic MITgcm).

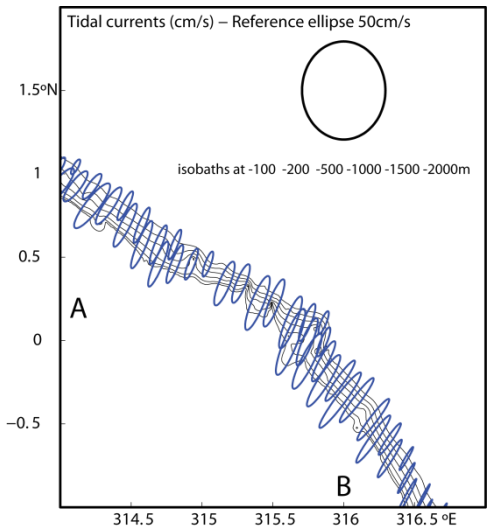

Figure R2. Ellipse tidal map computed from a least-square fit to the 1/12° regional tidal model OTIS run for one tidal cycle on 3 October 2011 (i.e. close to neap-tides). A 50 cm/s reference ellipse is also shown.

7. page 19, line 8: Shouldn't use 'precisely' here. This is not very precise. Why was a 30 m amplitude internal tide used? What if it was 25 m or 20 m?

R: We agree with the referee and will replace 'precisely' with 'approximately' in the new version of the manuscript. The nominal value for the IT amplitude was inferred from Vlasenko et al. (2005) and their Fig. 3.3, which shows low frequency internal oscillations measured in the study region with amplitude of approximate 30 m. We acknowledge that this value may change between generation sites and amongst different seasons, hence changing the overall agreement between the ISW observations and the disintegration envelope in Fig. 12b. However, we note that the key parameter governing nonlinearity in Fig. 12b is the thermocline thickness (i.e. *Ht* in Fig. 12a), and in this case the agreement between SAR and climatological data would still remain – i.e. ISWs are only observed after ITs propagate along an increasingly narrow pycnocline where nonlinearity effects increase significantly.

8. For several of the figures the labelling of the horizontal axis could be improved. For example in Figure 5 'km' appears directly under the fifth column. It would be better to have the number 300 there with 'km' below the numbers along the axis. Several other figures have this problem.

R: Axis on Figs. 4 to 7 where edited as suggested by the referee (see attached files). However, we note that on some occasions (e.g. SAR images) axis are labelled in order to optimize the area available for figure contents (usually small in printed versions), which should appear as large as possible (see e.g. Fig. 3).

9. The caption for Figure 12 should say what the different coloured curves are for and what the solid vs dashed lines are for. It would seem better to change the vertical scales for panels (c) and (d) to zoom in, although really I don't see that these figures are necessary. The values for the two dispersion parameters are discussed in the text and I don't see that these figures add anything. It would be helpful to indicate 1° and 3° N along the axis and perhaps distances.

R: A new version of Fig. 12 follows below, along with a new figure caption, according to the referee's suggestions. Additional labels were added to panels (c) and (d) in order to illustrate characteristic ocean values for dispersion as compared to typical values in the study region, and hence we prefer to keep these for consistency. Also, distances could not be added to Fig. 12 since three different wave paths are depicted in each panel (corresponding to different colours, see also Fig. 9), which would necessarily translate into three different distance axes (whereas latitude may be used as a common reference).

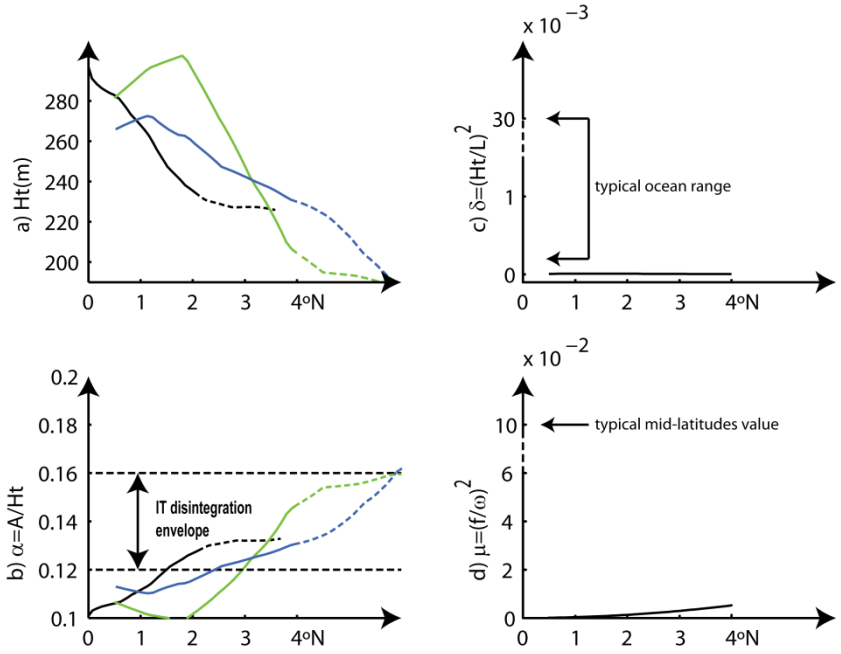

New Fig. 12. (a) Vertical extension of the waveguides calculated along the waves' propagation paths (in green, blue and black, according to dashed propagation paths in Fig. 9). (b) Same as panel (a) for the nonlinear parameter computed assuming an IT amplitude of 30 m. (c) Nonhydrostatic dispersion for L = 100 km. (d) Rotational dispersion for the semi-diurnal IT. Transitions to dashed lines in left panels indicate first SAR evidences of ISWs. Note broken vertical axes in right panels and typical ocean values showing comparatively week dispersions in our study region. See text for more details.

10. It would help if distances were included in Figure 11 instead of just latitude. The difference in stratification between profiles P1 and P2 doesn't seem to be very large. Perhaps show some N profiles at some higher latitudes. What is the stratification like closer to shore or does figure go to the 500 depth contour?

R: Distances along the horizontal axis are now included in a new version of Fig. 11 (see attached files). Profiles P1 and P2 have been selected as representative of the waveguide at the shelf-break (depicted between the 200 and 1000m in the new version of Fig. 9) and just prior to ISW evidence seen from SAR (respectively). While the emphasis is on the waveguide narrowing, which is best seen in the density contours (in left panel), these profiles add additional information showing that the pycnocline (in yellow colours) is brought closer to the surface and slightly reinforced. We agree, however, that these differences are indeed not very large as the referee points out, which may be a consequence of their climatological (and hence averaged) nature, just as for the horizontal currents discussed in section 3.1. We also note that profiles to the north of P2 (thus farther offshore of the ISWs earliest evidences) would actually reveal an even stronger pycnocline, while the shallowing effect would be lost (cf. yellowish colours in left panel go deeper as they move further offshore). Nonetheless, the waveguide vertical decreasing is well depicted in Fig. 11a and in good agreement with SAR observations, whereas larger variations in stratification profiles may be appreciated from the in situ measurements shown in Fig. 3.2c in Vlasenko's et al. (2005). While slightly westwards of the ISWs propagation paths (considering site A, see our Fig. 1), their measurements reveal changes in the pycnocline depth of the order of 100 m as it shallows in the offshore direction. Finally, depth contours for 200, 500, and 1000 m are practically coincident and representative of a very narrow shelf-break (see new Fig. 9), where the IT waves are believed to be generated (see also our Fig. 10). The 500 m contour was therefore taken as representative of the shelf-break and used as an onshore limit for Fig. 11a – past which the climatological stratification used in this case would illustrate on-shelf conditions, which do not concern the offshore propagating ITs and associated ISWs observed in deep ocean.

11. Page 12, line 12. The current often looks to be more in the direction normal to that of wave propagation, not in the opposite direction.

R: We again agree with the referee, whereas currents in May flow approximately in the opposite direction of those seen in October, and not directly against the ISWs mean propagation path. This will be changed in the text accordingly.

12. Does the Amazon river outflow make any contribution to the observed phenomena? For example surface currents, setting the stratification? What is the cause of the offshore thinning of the stratified layer? Is it simple geostrophic balance with the Brazilian current or does the Amazon river plume have anything to do with it?

R: We appreciated the referee's suggestion, but in this particular case the Amazon River outflow is unlikely to influence the ISWs dynamics, setting neither their near-surface currents

nor their stratification. Typically a NW Amazon plume is observed to develop and extend westward of 47° W (regardless of the wind regime, since it is the NBC the primary forcing term), and hence not necessarily related with the ISWs shown in our Fig. 1, which are eastwards of 46° W (see e.g. Figs. 10 and 13 in Nikiema et al., 2007, and references therein). As the referee suggests the offshore thinning of the waveguide is related to the NBC and the NECC, which are assumed to be in geostrophic and hydrostatic balance along the waves propagations paths (i.e. as they move increasingly far from the equator), and therefore in agreement with the thermal wind (shear) equation, which governs large-scale circulations in the ocean. When changing temperature for density, a relation between horizontal density gradients and vertical sheared flow may then be written as:

$$\frac{\partial \overrightarrow{u_g}}{\partial z} = -\frac{g}{f\rho_0}\hat{z} \times grad(\rho),$$

where $\boldsymbol{u_g}$ is the geostrophic velocity vector (in the zonal and meridional directions, and z is the vertical coordinate), g is the acceleration due to gravity, f the Coriolis parameter, ρ is the background density and ρ_0 some reference value. According to this relation, density changes in the horizontal are intertwined with geostrophic current variations in the vertical (i.e. shear). In particular, Fig. R3 shows how this translates to our study region where the NCB flows westwards, and the NECC flows either eastwards in October, or also westwards in May (but with much weaker currents). The density section (in light red) begins with a thicker waveguide at lower latitudes, owing to the negative vertical shear of the westward NBC (see also Johns et al., 1998) which holds at about 3°N (see also a surface map for the North Brazilian Current here http://oceancurrents.rsmas.miami.edu/atlantic/north-brazil_3.html). Between the NBC and the NECC a thinner waveguide is seen to develop and extend northwards, resulting from either a weaker westward NECC in May, or even a strong eastward NECC in October (in green and blue arrows in Fig. R3).

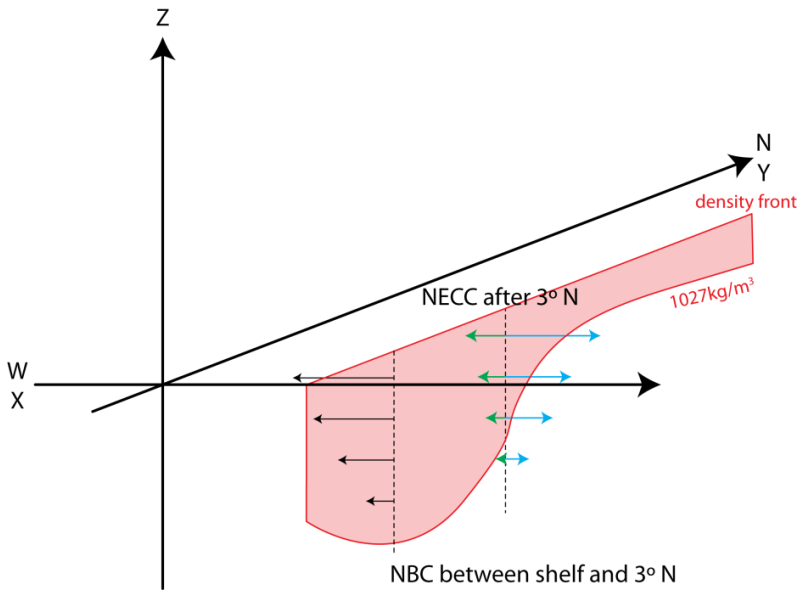

Figure R3. In the y–z plane a density front is seen towards north, representative of that seen in our Fig. 11, where isopycnals (see e.g. the 1027 kg/m^3 red line) are first seen slightly falling and then raising substantially, meaning that at some depth z, the density is first decreasing and then increasing with increasing latitude. According to the thermal wind equation, the zonal velocity must therefore first decrease in the vertical as seen in the NBC (in black arrows), and then decrease to a less extent or even increase with z as seen in the NECC (for May in green and October in blue, respectively).

Additional references (not included in the main text):

Araújo, I.B., da Silva, J.C.B., Ermakov, S.A., Robinson, I.S., 2002. On the role of wind direction in ERS SAR signatures of internal waves on the Iberian Shelf. Global Atmos. Ocean Syst. 8 (4), 269–281.

Brandt, P., Romeiser, R., Rubino, A., 1999. On the determination of characteristics of the interior ocean dynamics from radar signatures of internal solitary waves. J. Geophys. Res. 103, 8009–8031, http://dx.doi.org/10.1029/1999JC900092.

W. E. **Johns**, T. N. Lee, R. C. Beardsley, J. Candela, R. Limeburner, and B. Castro, 1998: Annual Cycle and Variability of the North Brazil Current. J. Phys. Oceanogr., 28, 103–128. doi: http://dx.doi.org/10.1175/1520-0485(1998)028<0103:ACAVOT>2.0.CO;2

Oumarou **Nikiema**, Jean-Luc Devenon, Malika Baklouti, Numerical modeling of the Amazon River plume, Continental Shelf Research, Volume 27, Issue 7, 1 April 2007, Pages 873-899. Doi: 10.1016/j.csr.2006.12.004.

Kudryavtsev, V., D. Akimov, J. Johannessen, and B. Chapron (2005), On radar imaging of current features: 1. Model and comparison with observations, J. Geophys. Res., 110, C07016, doi:10.1029/2004JC002505.